EXPERIMENTAL RESULTS ON QCD AND JETS AT LEP AND SLC *

SIEGFRIED BETHKE
III. Phys. Institut, RWTH Physikzentrum
D - 52056 Aachen, Germany
E-mail: SIGGI @ CERNVM.bitnet

ABSTRACT

A selection of results from e^+e^- annihilations at c.m. energies around the Z^0 resonance, testing the predictions of perturbative Quantum Chromodynamics, is presented. Measurements of the strong coupling strength, α_s, are updated and reviewed, and a world compilation of α_s determinations is given. Determinations of the QCD gauge group constants from 4- as well as from 2- and 3-jet events are summarised. Model independent studies of the properties of identified quark and gluon jets and results of sub-jet multiplicities of 2- and 3-jet events are presented. The first comparison of the structure of jets from e^+e^- annihilation and from $p\overline{p}$ collisions is discussed.

1. Introduction

The large electron-positron colliders LEP and SLC, which operate at the highest available energies in e^+e^- annihilation, have provided a wealth of precise studies of hadronic final states and, more specifically, of Quantum Chromodynamics (QCD), the theory of the strong interactions. The unprecedented precision of these studies is basically due to the large cross section at the Z^0 resonance, and thus to the large data statistics which was accumulated in the past, especially at LEP where each experiment has collected about 2 million hadronic Z^0 decays. In addition, the high centre of mass energy provides a closer relationship between hadron jets and the underlying partons (i.e. quarks and gluons) than at previous e^+e^- colliders.

About sixty QCD-related publications are available from the four LEP experiments ALEPH, DELPHI, L3 and OPAL; a smaller number of QCD publications is also available from the experiments at the SLC linear collider, MARK-II and SLD. The following topics have been extensively covered:

- studies of the general properties of hadronic final states, like event shape distributions, fragmentation functions and multiplicities of various types of particles, intermittency and Bose-Einstein correlations;
- determinations of the coupling strength, α_s, from a large variety of observables;
- studies of 3-jet events, which provide evidence for asymptotic freedom and lead to tests of the QCD 3-jet matrix element, to observations of quark-gluon jet differences and of the string hadronisation effect;

*Talk presented at the Tennessee International Symposium on Radiative Corrections, Gatlinburg USA, June 27 - July 1, 1994

- studies of 4-jet events in order to proof the nonabelian gauge structure and to verify the colour factors of the theory;
- studies of soft gluon coherence effects.

This review will concentrate on a summary of measurements of α_s at LEP/SLC and a world compilation of α_s results (Section 2), on tests of the gauge group structure of QCD (Section 3), on a study of differences between quark and gluon jets (Section 4), on studies of sub-jet multiplicities of 2- and 3-jet events and a comparison of jets observed in e^+e^- annihilation and in $p\bar{p}$ collisions (Section 5). Future aspects will be discussed in Section 6. A general introduction to the field and a more complete selection of topics can be obtained from previous reviews [1-6].

2. Measurements of α_s at LEP and SLC

2.1. $\alpha_s(M_{Z^0})$ from Hadronic Event Shapes, Energy Correlations and Jet Rates

Hadronic event shape variables are tools to study both the amount of gluon radiation and details of the hadronisation process. The definitions of observables which are applied to hadronic final states of e^+e^- annihilations, like Thrust, Thrust major and minor, Oblateness, Sphericity, Aplanarity, jet masses, the jet broadening measures, energy correlations and jet production rates, are summarised elsewhere [6]. Many of the observables are, to some degree, correlated with each other. In leading order ($\mathcal{O}(\alpha_s)$) QCD, some are even identical; however the higher order QCD corrections are different, in general.

2.1.1. $\alpha_s(M_{Z^0})$ Using QCD Calculations to Complete $\mathcal{O}(\alpha_s^2)$

Typically, all the observables studied in determinations of α_s are calculated to complete $\mathcal{O}(\alpha_s^2)$ perturbation theory [7], for massless quarks and gluons. To this order, the differential distribution of an observable y is given in the form

$$\frac{1}{\sigma_0}\frac{d\sigma}{dy} = \frac{\alpha_s(\mu)}{2\pi}A(y) + \left(\frac{\alpha_s(\mu)}{2\pi}\right)^2 [A(y)2\pi\beta_0 \ln(x_\mu^2) + B(y)], \tag{1}$$

where σ_0 is the lowest (0th) order cross-section for e^+e^- annihilation into hadrons, $\beta_0 = 11 - 2N_f/3$, $x_\mu = \mu/E_{cm}$ is the renormalisation scale factor, and $A(y)$, $B(y)$ are functions depending on the specific variable. The next-to-leading and higher order coefficients of α_s depend on the choice of the renormalisation scale μ which is not unambiguously defined by the theory, and also on the choice of the renormalisation scheme[†]. This imposes theoretical uncertainties which only vanish in *exact*, i.e. infinite order expressions. The scale dependence of results in truncated order of perturbation theory is thus a measure of the unknown higher order contributions.

[†]Physics analyses in e^+e^- annihilation generally refer to the $\overline{\mathrm{MS}}$ renormalisation scheme [8].

In recent studies, the size of higher order uncertainties is verified by analysing many different observables in a consistent study of one event sample, from one experiment [9,10]. Note that within the experimental errors of typically 1% to 3% in α_s, the results from different observables do not agree with each other [10]. In order for those results to be compatible it is mandatory that theoretical uncertainties must be considered, too [10,6].

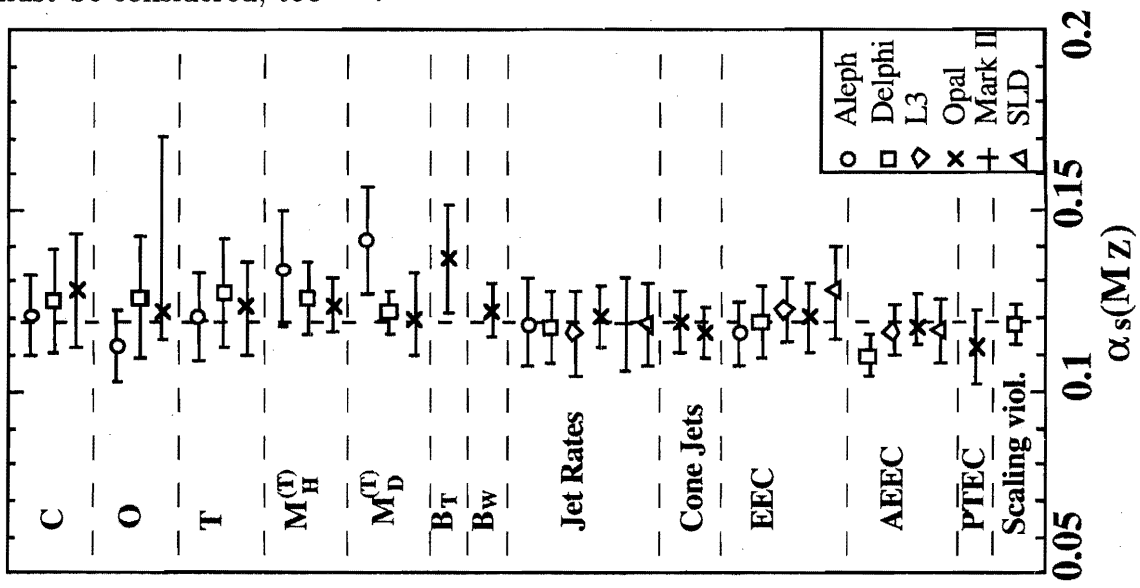

Figure 1. Compilation of measurements of $\alpha_s(M_{Z^0})$ from event shapes, jet rates and energy correlations, in $\mathcal{O}(\alpha_s^2)$, at LEP and SLC. The errors contain the experimental and theoretical uncertainties, added in quadrature.

An update of the results of $\alpha_s(M_{Z^0})$ in $\mathcal{O}(\alpha_s^2)$ QCD, from all experiments at LEP and SLC, is presented in Figure 1. Good agreement is found between the experiments, but note that the errors are largely dominated by theoretical uncertainties, which are common to all the experiments. The overall combined result is

$$\alpha_s(M_{Z^0}) = 0.119 \pm 0.006 \ ,$$

whereby the final error was taken from estimates of the overall remaining, uncorrelated uncertainties [9,10].

2.1.2. $\alpha_s(M_{Z^0})$ Using Resummed $\mathcal{O}(\alpha_s^2)$ QCD Calculations

Since calculations which are based on $\mathcal{O}(\alpha_s^2)$ matrix elements usually are unsuccessful in describing the back-to-back two-jet region of phase space, an alternative approach is taken which is based on the resummation of leading logarithms arising from soft and collinear singularities in gluon emission. In resummed calculations, the effective expansion parameter is not α_s, but $\alpha_s L^2$ (to leading order in L), where $L = \ln(1/y)$ and y is some generic observable which tends to zero in the two-jet region. At small y the value of $\alpha_s L^2$ is not small, and therefore these terms must be

summed to all orders in α_s in order to provide a satisfactory calculation. For certain observables it has proved possible to sum both the leading and next-to-leading logarithms, which is referred to as the 'Next-to-Leading Log Approximation' or NLLA [11].

If the maximum available information from both NLLA and $\mathcal{O}(\alpha_s^2)$ calculations shall be utilised, they must be added such that double counting of those terms which are common to both these calculations is avoided. This can be done involving several (approximate), so called 'matching schemes'. Different matching schemes can yield different values of α_s in experimental analyses, and thus may contribute as another source of theoretical uncertainties.

Resummation is expected to provide more accurate predictions of the distributions, especially at high thrust or low jet masses. Their dependence on the renormalisation scale should also be reduced if compared to pure $\mathcal{O}(\alpha_s^2)$ calculations. Both these expectations were confirmed in experimental studies [12,13].

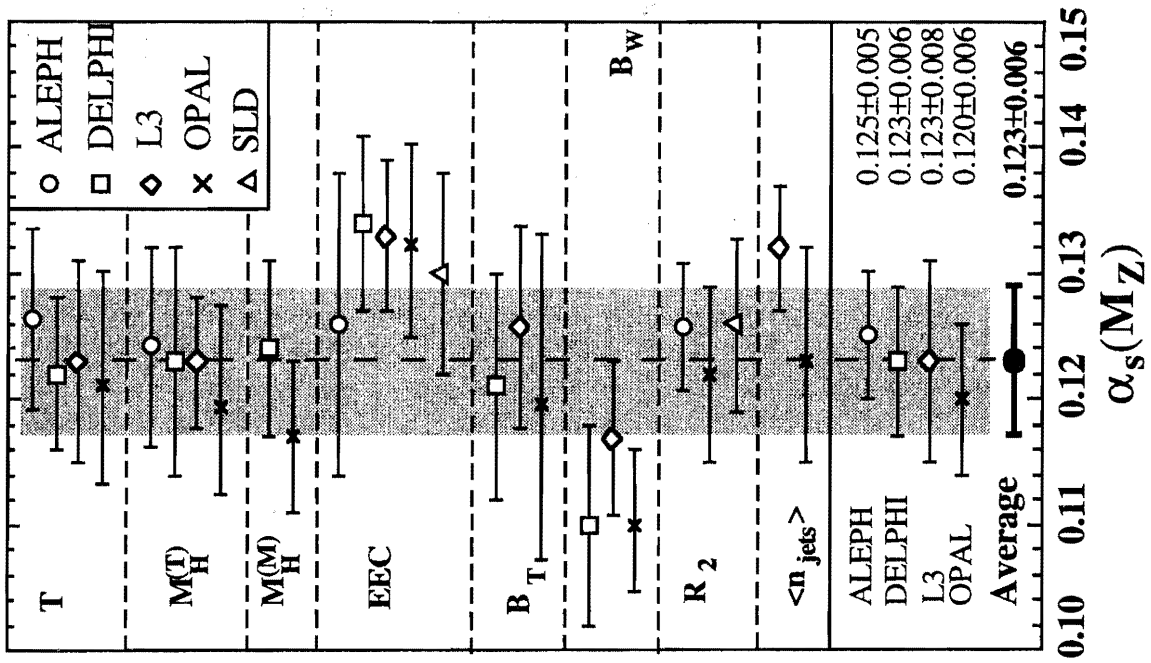

Figure 2. Summary of measurements of $\alpha_s(M_{Z^0})$ from LEP and SLC, using resummed $\mathcal{O}(\alpha_s^2)$ QCD calculations.

A summary of $\alpha_s(M_{Z^0})$ from resummed calculations is given in Figure 2. In contrast to the results in $\mathcal{O}(\alpha_s^2)$ QCD (*c.f.* Figure 1), the central values of $\alpha_s(M_{Z^0})$ are always given for $\mu = E_{cm}$, since small renormalisation scales are no longer preferred in resummed calculations. In fact, best fit results are obtained for renormalisation scales much closer to $\mu = E_{cm}$ than in the case of $\mathcal{O}(\alpha_s^2)$ QCD. Nevertheless, an uncertainty in α_s due to the detailed choice of the renormalisation scale, usually taking $\frac{1}{2} \leq x_\mu \leq 2$, is still present in resummed $\mathcal{O}(\alpha_s^2)$, which is however smaller than in $\mathcal{O}(\alpha_s^2)$ alone.

The errors presented in Figure 2 include experimental and theoretical (i.e. mainly

scale) uncertainties, added in quadrature. Combining these results provides an average value of

$$\alpha_s(M_{Z^0}) = 0.123 \pm 0.006 \ .$$

2.2. $\alpha_s(M_{Z^0})$ From the Hadronic Width of the Z^0

A reliable way to determine $\alpha_s(M_{Z^0})$ is a precise measurement of the ratio R_Z of the hadronic and electronic partial widths of the Z^0,

$$R_Z \equiv \left(\frac{\Gamma_{\rm had}}{\Gamma_{e^+e^-}}\right)_{\rm exp} = \left(\frac{\Gamma_{\rm had}}{\Gamma_{e^+e^-}}\right)_0 (1 + \delta_{\rm QCD}) \, , \tag{2}$$

since it is not affected by hadronisation effects and because the QCD correction $\delta_{\rm QCD}$ has been calculated to complete third order ($O(\alpha_s^3)$) perturbation theory [14]. Including all recently calculated electroweak and QCD corrections as well as heavy quark mass effects, $\delta_{\rm QCD}$ is of the form [15]

$$\delta_{\rm QCD} = 1.06 \left(\frac{\alpha_s}{\pi}\right) + 0.9 \left(\frac{\alpha_s}{\pi}\right)^2 - 15 \left(\frac{\alpha_s}{\pi}\right)^3 . \tag{3}$$

The expectation for $(\Gamma_{\rm had}/\Gamma_{e^+e^-})_0$, without QCD corrections, is 19.943, for masses of the top quark and of the Higgs particle of $M_t = 150$ GeV and $M_H = 300$ GeV, respectively [15]. The uncertainties of this parametrisation, including variations of M_t from 100 to 200 GeV and of M_H from 60 to 1000 GeV as well as higher order QCD uncertainties, are estimated to be

$$\Delta\alpha_s = \pm 0.002 \text{ (electroweak) } \pm 0.002 \text{ (QCD) } {}^{+0.004}_{-0.003} \, (M_t, \ M_H) \ = \ {}^{+0.005}_{-0.004} \ . \tag{4}$$

The preliminary, updated average value of R_Z, summarised from the measurements of the four LEP experiments and partly including the new data from the 1993 run, is [16] $R_Z = 20.789 \pm 0.040$. This is based on a total of about 7.4×10^6 hadronic and 8×10^5 leptonic Z^0 decays. From this result one infers $\alpha_s(M_{Z^0}) = 0.124 \pm 0.006^{+0.005}_{-0.004}$, where the first error is statistical and the second is the theoretical uncertainty given above. Adding these errors in quadrature results in

$$\alpha_s(M_{Z^0}) = 0.124^{+0.008}_{-0.007} \ ,$$

which is in perfect agreement with the measurements from hadronic event shapes, jet rates and energy correlations.

From a combined fit of M_t and $\alpha_s(M_{Z^0})$ to all LEP data on hadronic and leptonic Z^0 line shapes and measurements of lepton and quark asymmetries [17], one obtains $M_t = 165^{+13+18}_{-14-19}$ GeV and $\alpha_s(M_{Z^0}) = 0.125 \pm 0.005 \pm 0.002$, where the first error is experimental and the second is due to the unknown mass of the Higgs boson. The additional renormalisation scale dependence of α_s in these fits is about ± 0.003, for $x_\mu = 0.5 \ldots 2$.

2.3. α_s From τ Decays

The ratio R_τ of the hadronic and electronic branching fractions of the τ lepton,

$$R_\tau = \frac{B(\tau \to \text{hadrons} + \nu_\tau)}{B(\tau \to e\bar{\nu}_e\nu_\tau)} \equiv \frac{1 - B_e - B_\mu}{B_e}, \tag{5}$$

which can be reliably determined by measurements of the electronic and muonic branching fractions B_e and B_μ, is theoretically expected to be given by [18]

$$R_\tau = 3.058(1.001 + \delta_{\text{pert}} + \delta_{\text{nonpert}}) \ . \tag{6}$$

Here, δ_{pert} and δ_{nonpert} are perturbative and non-perturbative QCD corrections; δ_{pert} was calculated to complete $\mathcal{O}(\alpha_s^3)$ and is of similar structure as the one for R_Z [18,19]. The non-perturbative correction was estimated to be small [18], $\delta_{\text{nonpert}} = -0.007 \pm 0.004$.

The average value, combined from the four LEP experiments [20], is $R_\tau = 3.617 \pm 0.034$, which leads to $\alpha_s(M_\tau) = 0.360 \pm 0.04$, in $\mathcal{O}(\alpha_s^3)$. This result, which also contains a renormalisation scale uncertainty of ± 0.03, added in quadrature, is significantly larger than the value of $\alpha_s(M_{Z^0})$ from event shapes and jet rates measured in Z^0 decay, as expected by QCD.

A new method of analysis was proposed, in which δ_{nonpert} can be simultaneously determined from the data [21], in addition to $\alpha_s(M_\tau)$, instead of relying on the estimates of δ_{nonpert} mentioned above. This method requires the measurement of weighted integrals of the hadronic invariant mass spectrum of τ decays. The ALEPH collaboration has contributed an analysis [22] which is based on this new method and on improved QCD predictions. The result is $\alpha_s(M_\tau) = 0.330 \pm 0.046$, which is in good agreement with the result (0.360) given above and therefore indicates that nonperturbative corrections to R_τ are indeed very small: the ALEPH fit gives $\delta_{\text{nonpert}} = 0.003 \pm 0.005$.

When extrapolating this value of α_s from $\mu = M_\tau$ to $\mu = M_{Z^0}$, $\Lambda_{\overline{MS}}$ must change when crossing a quark threshold [23,24]. This results in

$$\alpha_s(M_{Z^0}) = 0.122 \pm 0.005$$

from τ decays at LEP, where the relative size of the error is decreased because of the logarithmic dependence of α_s on μ. The agreement with $\alpha_s(M_{Z^0})$ obtained from hadronic event shapes and from R_Z is remarkable, especially if one considers the large difference in the effective energy scale. This agreement may be one of the most important QCD tests performed at LEP so far!

2.4. World Summary of α_s Measurements

A world summary of α_s measurements, updated from previous compilations [6,25], is presented in Figure 3. The values of α_s are given at typical energy scales Q where

actual measurements were done. The errors contain experimental and theoretical uncertainties, added in quadrature. The symbols indicate the type of QCD perturbation theory used to determine α_s, where 'Lattice' means lattice gauge theory, and (N)NLO stands for (next-to-)next-to-leading order perturbation theory.

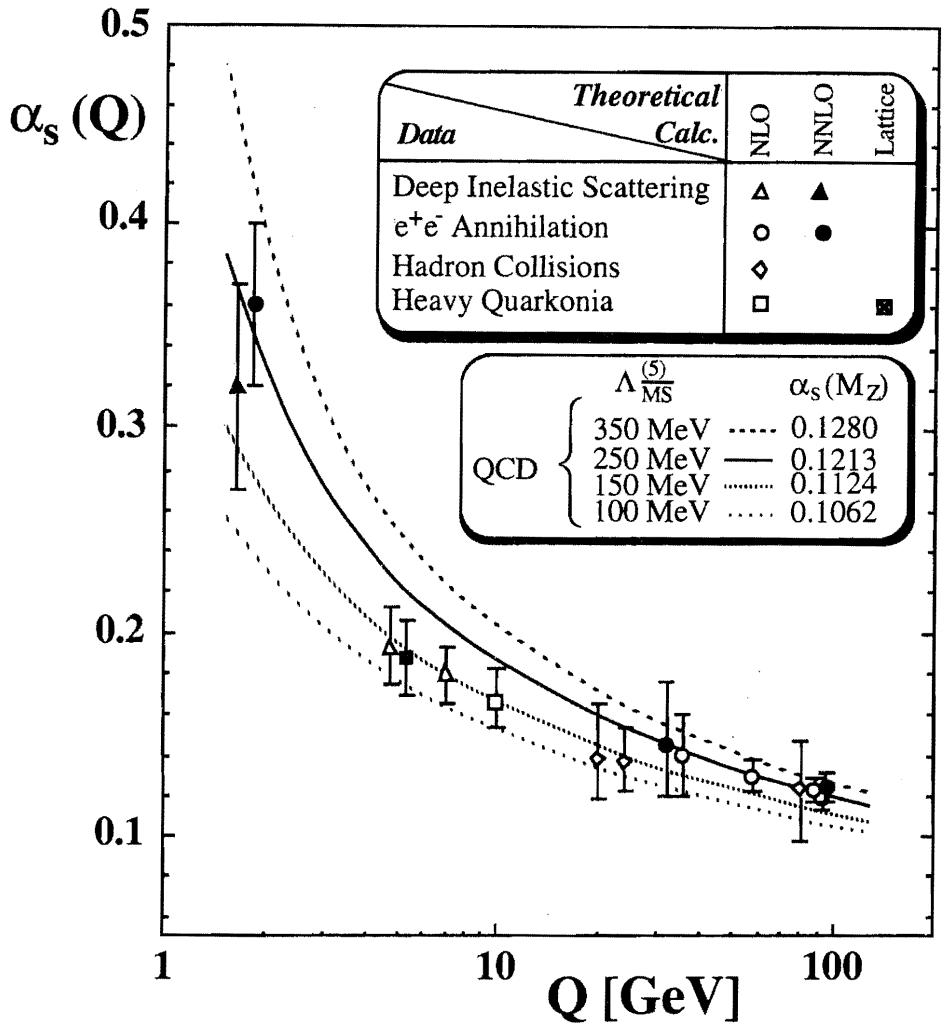

Figure 3. A Summary of measurements of α_s, compared with QCD expectations for four different values of $\Lambda_{\overline{MS}}$ which are given for the region where $N_f = 5$ (i.e. $Q \geq 10$ GeV).

There is significant evidence for the running of α_s. The data are compared with the QCD predictions of a running coupling constant, calculated in $\mathcal{O}(\alpha_s^3)$ for four different values of $\Lambda_{\overline{MS}}$ which are given for $N_f = 5$ quark flavours. The energy dependence of α_s is distinct, and is in very good agreement with the QCD prediction. In fact, significant evidence for the running of α_s comes from LEP alone, which provides precision results at the smallest and at the largest available energies, based on the highest calculated order of QCD perturbation theory, $\mathcal{O}(\alpha_s^3)$.

Small systematic differences between different results appear to be visible, however: the lower energy results from deep inelastic scattering and from quarkonia

decays, but *not* those from R_τ, seem to prefer smaller values of $\Lambda_{\overline{MS}}$ than those from LEP and SLC. Possible explanations for this systematic difference will be discussed in more detail in a forthcoming review [26], which will also contain several new (preliminary) results which became available only shortly after this conference.

Forming a weighted average of the results shown in Figure 3, now *including* the new result from lattice gauge theory [27], one obtains $\alpha_s(M_{Z^0}) = 0.117$ as the central value[‡] Since the errors of most results are mainly due to theoretical uncertainties, the final error of the overall combined value of $\alpha_s(M_{Z^0})$ cannot be obtained by using standard techniques of error calculation. We therefore take as the overall, final error on $\alpha_s(M_{Z^0})$ the typical uncertainty from the most reliable individual α_s determinations, $\Delta\alpha_s(M_{Z^0}) = \pm 0.006$. The world average is thus quoted to be

$$\alpha_s(M_{Z^0}) = 0.117 \pm 0.006 \ ,$$

which corresponds, in $\mathcal{O}(\alpha_s^3)$ and for $N_f = 5$ or 4 quark flavours, to

$$\Lambda_{\overline{MS}}^{(5)} = 195^{+80}_{-60} \text{ MeV}, \text{ or } \Lambda_{\overline{MS}}^{(4)} = 280^{+95}_{-80} \text{ MeV} \ .$$

3. Tests of the Gauge Group Structure of QCD

The nonabelian nature of QCD manifests itself in the characteristic running of α_s with energy and in the process of gluon self coupling. While evidence for asymptotic freedom is seen from the relative production rates of 3-jet events in e^+e^- annihilation [6], the kinematics of 4-jet final states provide the possibility to directly "see" the triple gluon vertex (TGV). About 95% of all 4-jet events are expected to be due to $q\bar{q}gg$ (i.e. double gluon bremsstrahlung and TGV) final states and only 5% are $q\bar{q}q\bar{q}$ (from $g \to q\bar{q}$ splitting) events [28]. An abelian model, in which the TGV does not exist and which can be constructed by simply replacing the group constants of SU(3), C_f, $C_A = N_c$ and T_f, with those of a suitable U(1) [29], predicts significantly different numbers, as can be seen from Table 1.

The different spin structure of the processes $g \to gg$ and $g \to q\bar{q}$ gives rise to different angular correlations within 4-jet events, which may be used to discriminate between QCD and the abelian scapegoat model. OPAL [30] and L3 [31] have studied the distributions of two such angles defined by the axes of reconstructed 4-jet events, which are especially sensitive to the relative contribution of $q\bar{q}q\bar{q}$ final states. The data are well described by the predictions of QCD, while abelian vector models fail to reproduce the shape of the data distribution.

DELPHI [32] and ALEPH [33] have studied more-dimensional distributions of various observables, which provides more direct evidence for the existence of the TGV. In fits of the $\mathcal{O}(\alpha_s^2)$ (i.e. leading order) 4-jet matrix element to their experimental distributions, both DELPHI and ALEPH determine the group constants N_c/C_f

[‡]With the inclusion of the newest results on α_s, the world avarage value of $\alpha_s(M_{Z^0})$ will change by less than 1% [26].

	QCD	abelian
C_f	4/3	1
N_c	3	0
T_f	1/2	3
$q\bar{q}gg$	$\approx 95\%$	$\approx 68\%$
$q\bar{q}q\bar{q}$	$\approx 5\%$	$\approx 32\%$

Table 1. Group constants of QCD and of the abelian vector theory, as well as the expected relative fractions of 4-jet events from $q\bar{q}gg$ and $q\bar{q}q\bar{q}$ final states.

and T_f/C_f. Note that the TGV contribution is proportional to N_c, the numbers of colours, while the process of $g \to q\bar{q}$ is basically proportional to $T_f N_f$, where N_f is the number of quark flavours.

In a recent preliminary study, ALEPH [34] also reported a determination of the group structure constants from a study of 3-jet topology and 2-jet event production rates, where the TGV contributes through loop corrections. While the results from this new study are less accurate than those from 4-jet events, they strengthen the previous results from 4-jet events and provide slightly smaller uncertainties in a combined fit to all jet data.

Experiment	Data	N_c/C_f	T_f/C_f
DELPHI	4-jet events	2.12 ± 0.35	0.46 ± 0.19
ALEPH	4-jet events	2.24 ± 0.40	0.58 ± 0.29
ALEPH	2+3-jet evts.	4.49 ± 1.35	2.01 ± 0.99
ALEPH	2+3+4-jet evts.	2.43 ± 0.31	0.55 ± 0.23

Table 2. Fit results of the group constant ratios N_c/C_f and T_f/C_f.

The final results are compiled in Table 2, and the ALEPH data are also shown in Figure 4. The results are in good agreement with the expectations of QCD, while abelian models are significantly ruled out. In particular, the non-zero result for N_c/C_f is interpreted as direct evidence for the TGV.

4. Differences between Quark and Gluon Jets

In QCD, gluons are associated with a relative coupling strength $\propto N_C = 3$ while for quark this is $\propto C_F = 4/3$. At asymptotic jet energies and in leading order QCD, one thus expects a ratio of $(N_C/C_F) = 9/4$ for the multiplicity of soft gluons produced from the two jet types. For equal quark and gluon jet energies, this implies that the particle energy spectrum of the gluon jet should be softer (i.e. the particles from gluon jets have lower energies, on average). Also, since the mean transverse energy of particles w.r.t. the jet axis is expected to be about the same,

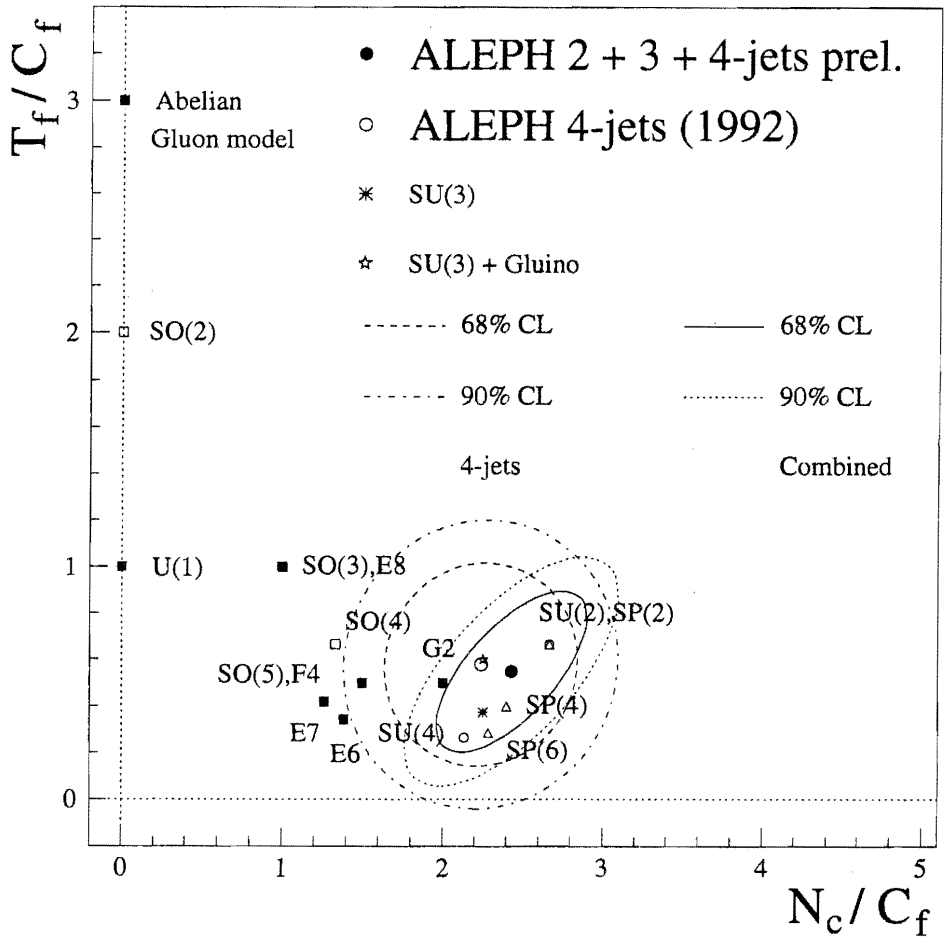

Fig. 4. Fit results and 68% and 90% confidence levels for the group constant ratios N_c/C_f and T_f/C_f, from studies of 4-jet events (dashed and dashed-dotted ellipses, respectively) and from 4- and 2+3-jet events combined (full and dotted ellipses, respectively). Data are from ALEPH. The values expected for QCD (SU(3)) and other gauge theories are indicated.

the angles of particles relative to their jet axes are expected to be larger in gluon jets, i.e. gluon jets are expected to be broader than quark jets.

The OPAL collaboration introduced a new method of tagging quark and gluon jets in symmetric 3-jet events, such that quark- and gluon-jets of roughly equal energy can be identified with a relatively high purity [35]. Symmetric 3-jet events are selected using the 'Durham' jet finder [36,37,38]. Only events with angles between the two lower energetic jets and the highest energy jet (called 'jet 1') of (150 ± 10) degrees are considered. Due to the bremsstrahlung nature of gluon radiation, jet 1 can then be identified as being a quark (or antiquark) jet, with a very high purity of about 97%. The two lower energy jets, having about equal energy, are thus known to be an equal mixture of quark and gluon jets; the averaged properties of these jets are thus defined to be those of a **'normal mixture'** jet. A subsample in which gluon jets are enriched is obtained by further selecting events in which a secondary vertex

is reconstructed in one of the two lower energetic jets. Such secondary vertices are due to the relatively long life time of bottom quarks ($\tau \sim 10^{-12}$ s). The other low energy jet is then taken to be the **'gluon tagged jet'**. With this method 1175 gluon jets with an average jet energy $\langle E_{jet} \rangle \sim 24$ GeV are selected.

The purity of the g-tagged jet sample is estimated to be about 80%, i.e. there is a contamination of about 20% quark jets in this sample. These numbers are obtained from a wide range of model studies, but also from the data themselves, using 3-jet events with two identified secondary vertex tags.

In a first step, the properties of 'g-tagged jets' are compared with those of 'normal mixture jets', i.e. one compares a sample of jets which consists of 80% gluons and 20% quarks with a set consisting of 50% quark and 50% gluon jets. No comparison with model calculations is necessary in this analysis. Also note that the tagged bottom quark jet is *not* used in this comparison, since b-quark jets have distinct properties, due to the heavy mass of this quark, which could bias the results.

The ratio of particle multiplicities n of these two jet samples amounts to

$$\frac{\langle n \rangle_{gluon-tagged}}{\langle n \rangle_{normal-mixture}} = 1.081 \pm 0.011 \ .$$

In addition, distributions of particle energies and angles w.r.t. the jet axes show that the gluon tagged jets are generally broader, and their particles are less energetic, on average.

Results for *pure* gluon and quark jet samples are obtained by unfolding the measured distributions according to the q- and g-contents of the two samples. The ratio of particle multiplicities in g- and in q-jets is then determined to be

$$\frac{\langle n \rangle_{\text{gluon}}}{\langle n \rangle_{\text{quark}}} = 1.27 \pm 0.04(\text{stat.}) \pm 0.06(\text{syst.}) \ .$$

This is significantly larger than unity, but is also lower than the naive expectation of 9/4 – which is however only valid in lowest order and for asymptotic jet energies. A value lower than 9/4 is indeed expected from higher order QCD calculations; however a direct prediction of the experimental number given above does not exist. The distributions of particle energies in gluon and in quark jets is shown in Fig. 5, demonstrating that gluon jets have a significantly softer energy spectrum than quark jets, as expected (without further specification) by QCD.

5. Internal Jet Structure

5.1. Sub-Jet Multiplicities

No theoretical predictions exist for the ratio of hadron multiplicities in experimentally accessible quark- and in gluon-jets; however, sub-jet multiplicities of 2- and of 3-jet events have been calculated in NLLA of QCD [39]. The idea is to define 3-jet and 2-jet event samples with the Durham [36,37,38] jet finder at a fixed value

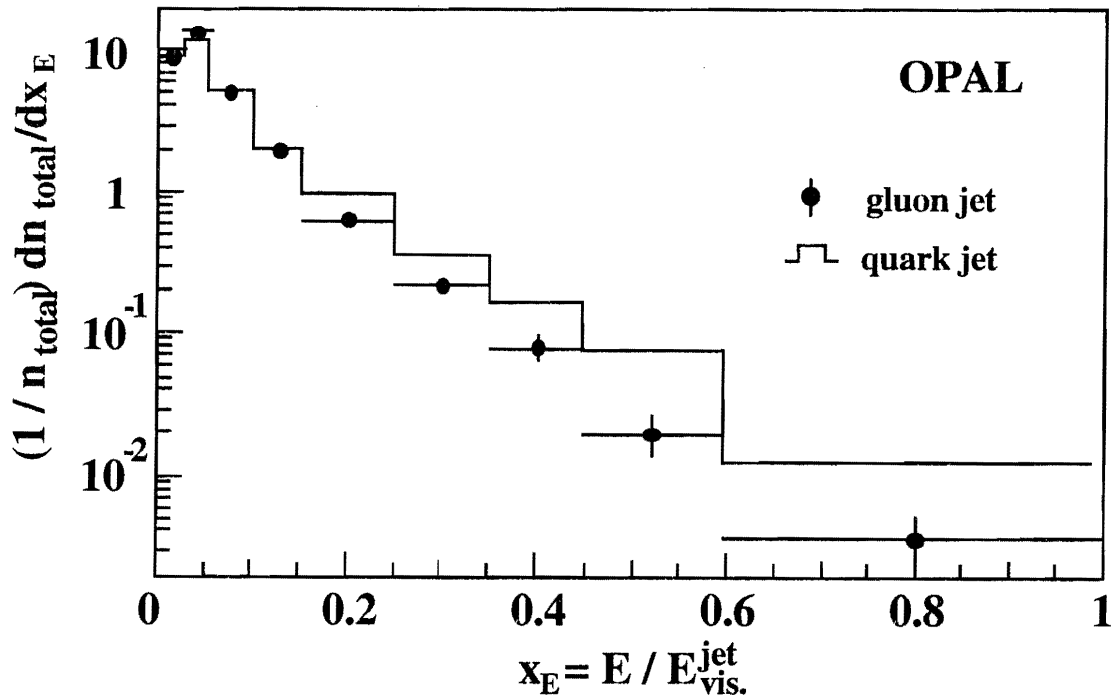

Figure 5. Scaled inclusive energy distributions of particles in gluon and in quark jets.

of the jet resolution parameter $y_{\rm cut} \equiv y_1$ ($y_{\rm cut}$ in this jet scheme is the minimum required, scaled transverse energy of one jet w.r.t. another, if both jets are to be resolved), and then to study the ratio of the average jet multiplicities of these two event classes, M_3/M_2, for decreasing jet resolution $y_0 < y_1$. In the limit of $y_0 \to 0$, one expects that

$$\frac{M_3}{M_2} \to \frac{2C_F + N_C}{2C_F} = \frac{17}{8} \, .$$

OPAL [40] has provided a new study of sub-jet multiplicities. In Figure 6, the data on M_3/M_2 are compared with the predictions of analytic QCD calculations, for different values of the QCD parameter Λ. At $y_1 = y_0 = 0.001$, the value of M_3/M_2 is (trivially) 3/2. Naively, this value should increase and approach the value of 17/8 for decreasing y_0. The data, however, rather decrease monotonically. With $\Lambda \sim$ 0.2 GeV, theory provides a reasonable description of the data down to $y_0 \sim 10^{-3}$, and then increases to eventually reach the value of 17/8. The region of $y_0 < 10^{-3}$ is presumably what is called the nonperturbative hadronisation regime, where the calculations are not supposed to be reliable. The fact that M_3/M_2 decreases for $y_0 < y_1$, however, is attributed to the effects of (destructive) interference of soft gluons within the calculations. This may also explain the result that the ratio of hadron multiplicity in gluon and in quark jets, as described in the previous section, is observed to be larger than unity by only 30%.

Comparisons of data with QCD plus hadronisation models reveal, in the same study of sub-jet multiplicities [40], that only those models which incorporate soft gluon interference effects *plus* string hadronisation can reproduce the data in the

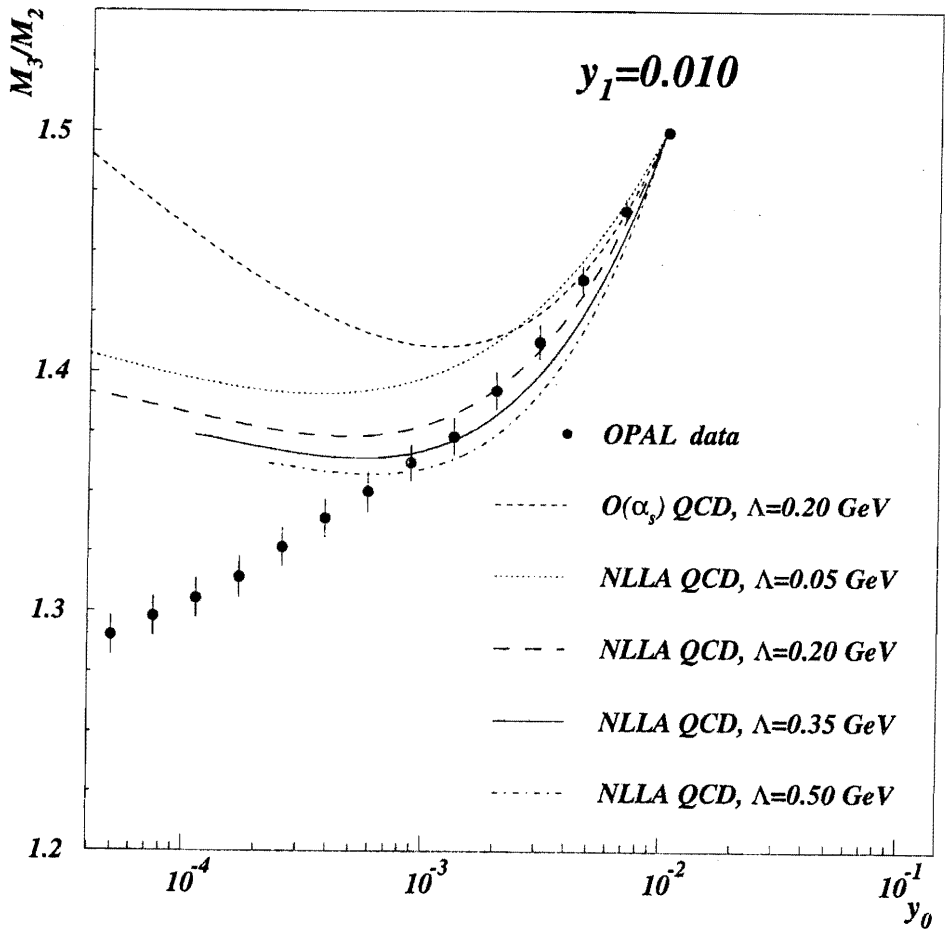

Figure 6. Ratio of sub-jet multiplicities of 3- and 2-jet events defined with a jet resultion $y_1 = 0.010$, compared with analytic QCD predictions in NNLA for different values of the QCD parameter Λ.

region of $y_0 < y_1$.

5.2. Comparison of e^+e^- *and* $p\bar{p}$ *Initiated Jets*

The OPAL collaboration has recently introduced a jet finding algorithm [41] for e^+e^- interactions which closely resembles the cone-based jet finders typically used in $p\bar{p}$ experiments. Cone-based jet finders are markedly different from jet cluster-algorithms [38] utilised in e^+e^- annihilation experiments. Therefore a direct comparison between properties of e^+e^- and $p\bar{p}$ generated jets was not possible so far. Apart from general investigations like jet production rates and a determination of $\alpha_s(M_{Z^0})$ (see Figure 1), based on the cone jet finder, OPAL compares jet energy profiles, i.e. the energy flow with respect to the jet axis, of e^+e^- jets with jets from $p\bar{p}$ initiated jets, measured by CDF [42].

In Figure 7, the differential energy flow $\Phi(r) = \frac{\Psi(r+\Delta r)-\Psi(r)}{\Delta r/R}$ is shown as a function of r, where $\Psi(r)$ is the fraction of energy inside a cone with half-angle r and the same

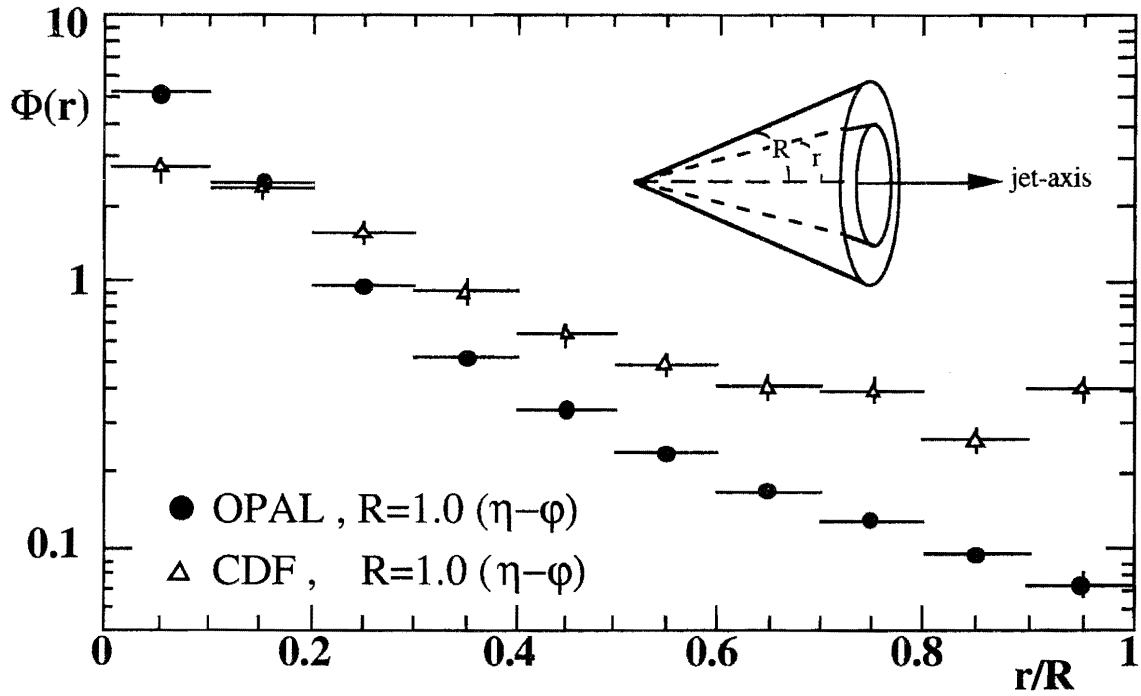

Figure 7. Differential energy profile for jets from e^+e^- annihilation (OPAL) and from $p\bar{p}$ collisions (CDF), using the same cone algorithm to define and reconstruct jets.

axis as the jet. The data are for jets defined by a cone half-angle R and jet energies $E_{jet} > 35$ GeV (OPAL) or 40 GeV $< E_\perp^{jet} <$ 60 GeV (CDF), respectively, averaging to similar values of $\langle E_{jet} \rangle \sim 45$ GeV and $\langle E_\perp^{jet} \rangle \sim 45$ GeV. It is found that jets in e^+e^- annihilation are significantly narrower than those observed in $p\bar{p}$ interactions. The influence of underlying events in the $p\bar{p}$ case was studied and found to explain only a small part of the differences seen. The difference must therefore be of dynamical origin; for example, the jets observed by OPAL are mostly induced by quarks, while those in the CDF data are supposed to originate mainly from energetic gluons. The differences observed in Figure 7 are thus likely to be due to the differences between quark- and gluon-jet fragmentation, as observed in the study of quark- and gluon-jet properties described above (c.f. Figure 5; for jets with mean jet energies of ~ 24 GeV).

6. Outlook and Future Requirements

Rather than summarising this short review of recent QCD studies performed at LEP and SLC, some of the future aspects and requirements for hadronic physics in e^+e^- annihilation, at current as well as at higher energies, shall be briefly discussed.

- **QCD with heavy quarks:** the large and still growing event statistics, together with excellent capabilities to tag b-quark jets by micro-vertex detectors, will allow to perform many interesting and precise studies in this field.

What is still needed, however, are the corresponding QCD calculations for *massive* quarks Q [$e^+e^- \to Q\overline{Q}g(g)$] in higher than leading order QCD.

- **α_s determination from event shapes, jet rates etc.:** More observables should be calculated in resummed $\mathcal{O}(\alpha_s^2)$ QCD, in order to further investigate (and possibly reduce) theoretical uncertainties. Even more important are calculations of jet cross sections (and/or of event shapes and energy correlations) in complete $\mathcal{O}(\alpha_s^3)$. If those existed for at least one or a few observables, the currently largest source of systematic uncertainties in NLO analyses could be verified, and possibly could also be reduced.

- **α_s determination from R_Z:** Since the calculations of QCD corrections to R_Z are by far the most advanced and most complete (in NNLO, including higher order mass terms, $O(\alpha\alpha_s)$ interference terms etc.), the precision of $\alpha_s(M_{Z^0})$ can only improve further by a decrease of the (still dominating) statistical error. The total error in $\alpha_s(M_{Z^0})$, however, is not likely to become smaller than $\Delta\alpha_s(M_{Z^0}) = \pm 0.005$, without precisely knowing the masses of the top-quark and of the Higgs-boson.

- **QCD group structure:** studies of 4-jet events are currently limited to the $\mathcal{O}(\alpha_s^2)$ QCD calculations, which is only the leading order for this process. Complete $\mathcal{O}(\alpha_s^3)$ matrix elements for 4-jet production are urgently needed in order to provide a reliable estimate of the theoretical uncertainties.

- **Gluon coherence, string effect, q/g differences:** Further calculations and predictions for experimentally feasible observables are desired.

Hadronic physics at LEP and SLC turned out to be very rich and successful: QCD is now tested to the level of about 5%, which is a remarkable precision in the field of strong interactions. The prospects for further improvements, as indicated in the list of future aspects above, put rather strong and well defined demands, mainly on further theoretical developments.

7. References

1. *Z Physics at LEP-I*, eds. G. Altarelli et al., CERN 89-08 (1989).
2. J. Drees, *Proc. of the "QCD – 20 Years Later" workshop at Aachen* (1992), World Scientific; WU B 92-31.
3. S. Bethke, *Proc. of the "QCD – 20 Years Later" workshop at Aachen* (1992), World Scientific.
4. T. Hebbeker, *Phys. Rep.* **217** (1992) 69.
5. S. Bethke and J. Pilcher, *Ann. Rev. Nucl. Part. Sci.* **42** (1992) 251.
6. S. Bethke, *Proc. Scottish Universities Summer School in Physics*, August 1993, St. Andrews; HD-PY 93/7.

7. P. Nason and Z. Kunszt [1].
8. W.A. Bardeen et al., *Phys. Rev.* **D18** (1978) 3998.
9. P. Abreu et al., DELPHI collab., *Z. Phys.* **C54** (1992) 55.
10. P.D. Acton et al., OPAL collab., *Z. Phys.* **C55** (1992) 1.
11. S. Catani et al., *Nucl.Phys.* **B407** (1993) 3.
12. P.D. Acton et al., OPAL collab., *Z. Phys.* **C59** (1993) 1.
13. P. Abreu et al., DELPHI collab., *Z. Phys.* **C59** (1993) 21.
14. S.G. Gorishny, A.L. Kataev and S.A. Larin, *Phys. Lett.* **B259** (1991) 144.
15. T. Hebbeker et al., *Phys. Lett.* **B331** (1994) 165.
16. P. Clarke, *Proc.* 29th *Rencontre de Moriond*, Meribel, France, March 12-19, 1994.
17. B. Pietrzyk, *Proc.* 29th *Rencontre de Moriond*, Meribel, France, March 12-19, 1994; LAPP-EXP-94-07.
18. E. Braaten, S. Narison and A. Pich, *Nucl. Phys.* **B373** (1992) 581.
19. F. Le Diberder and A. Pich, *Phys. Lett.* **B286** (1992) 147.
20. E. Fernandez, *Proc. of the 1993 EPS Conference*, Marseille; IFAE-93-001.
21. F. Le Diberder and A. Pich, *Phys. Lett.* **B289** (1992) 165.
22. D. Buskulic et al., ALEPH Collaboration, *Phys.Lett.* **B307** (1993) 209.
23. W. Bernreuther and W. Wetzel, *Nucl. Phys.* **B197** (1982) 228.
24. W.J. Marciano, *Phys. Rev.* **D29** (1984) 580.
25. S. Bethke, *Proc. XXVI Int. Conf. on HEP*, Dallas, Texas, August 1992; HD-PY 92/13.
26. S. Bethke, *Proc. of the QCD94*, Montpellier, France, July 7-13, 1994; Aachen preprint PITHA-94-30.
27. A.X. El-Khadra, *Proc.* 11th *Intern. Symp. on Lattice Field Theory*, Dallas, TX, 12-16 Oct 1993.
28. S. Bethke, A. Ricker and P. Zerwas, *Z. Phys.* **C49** (1991) 59.
29. G. Kramer, *Springer Tracts of Modern Physics* (1984) 102.
30. M.Z. Akrawy et al., OPAL collab., *Z. Phys.* **C49** (1990) 49.
31. B. Adeva et al., L3 collab., *Phys. Lett.* **B248** (1990) 227.
32. P. Abreu et al., DELPHI collab., *Z. Phys.* **C59** (1993) 357.
33. D. Decamp et al., ALEPH collab., *Phys. Lett.* **B284** (1992) 151.
34. D. Buskulic et al., ALEPH collab., *Contrib. to the* 27th *Int. Conf on HEP*, Glasgow 1994, Ref. 0525.
35. P.D. Acton et al., OPAL collab., *Z. Phys.* **C58** (1993) 387.
36. S. Catani et al., *Phys. Lett.*, **B269** (1991) 432.
37. N. Brown and W.J. Stirling, *Z. Phys.* **C53** (1992) 629.
38. S. Bethke, Z. Kunszt, D.E. Soper and W.J. Stirling, *Nucl. Phys.* **B370** (1992) 310.
39. S. Catani, B.R. Webber, Yu.L. Dokshitzer and F. Fiorani, *Nucl.Phys.* **B383** (1992) 419.
40. R. Akers et al., OPAL collab., CERN-PPE/94-52.
41. R. Akers et al. OPAL collab., *Z. Phys.* **C63** (1994) 197.
42. F. Abe et al., CDF collab., *Phys. Rev. Lett.* **70** (1993) 713.